

Ruthenium Nanoparticles Integrated Bimetallic Metal-Organic Frameworks Electrocatalysts for Multifunctional Electrode Materials and Practical Water Electrolysis in Seawater

Alagan Muthurasu¹, Kisan Chhetri¹, Bipeen Dahal¹, Hak Yong Kim^{1,2*}

¹Department of Nano Convergence Engineering, Jeonbuk National University, Jeonju 561-756, Republic of Korea

²Department of Organic Materials and Fiber Engineering, Jeonbuk National University, Jeonju 561-756, Republic of Korea

Corresponding Author's E-mail: khy@jbnu.ac.kr

1. Experimental section

1.1 Rotating disk electrode (RDE)

RDE analysis was carried out with the rotating speed of 100 - 2500 rpm, the prepared Ru MOF CoFe nanoarrays modified RRD working electrode was performed at a scan rate of 5 mV s⁻¹. Using Koutecky–Levich plots (J^{-1} vs. $\omega^{-1/2}$) the slopes were used to calculate at various electrode potentials. In the different potential ranges, the corresponding electrons transferred (n) number per O₂ molecule during the ORR process is calculated using the following Koutecky–Levich (K-L) equation.

$$\frac{1}{j} = \frac{1}{j_L} + \frac{1}{j_K} = \frac{1}{B\omega^{1/2}} + \frac{1}{j_K} \quad (1)$$

Where J is the measured current density, J_L is the kinetics current density, J_K is the diffusion-limited current density, ω is the electrode rotation rate (rad s⁻¹), and B could be calculated from the slope of the K-L plot based on the following Levich equation.

$$B = 0.62nFC_0(D_0)^{2/3}\nu^{-1/6} \quad (2)$$

$$j_K = nFkC_0 \quad (3)$$

F is the Faraday constant ($F = 96\,485 \text{ C mol}^{-1}$), C_0 is the bulk concentration of O_2 ($1.2 \times 10^{-6} \text{ mol cm}^{-3}$), D_0 is the diffusion coefficient of O_2 ($1.9 \times 10^{-5} \text{ cm}^2 \text{ s}^{-1}$), ν is the kinetic viscosity of the electrolyte ($0.01 \text{ cm}^2 \text{ s}^{-1}$), and k is the electron transfer rate constant.

1.2 Tafel calculation:

The mass-diffusion adjustment is often used to determine the Tafel slope's kinetic current density, which is dependent on the formula below:

$$J_K = \frac{J \times J_L}{J - J_L} \quad (4)$$

Where J is the measured current density, J_L and J_K are the kinetics and diffusion-limited current density, respectively.

1.3 Mass activity calculation:

The ORR mass activity (A g^{-1}) values were estimated from the catalyst loading m ($0.2 \text{ mg cm geo}^{-2}$) and the observed current density j (mA cm geo^{-2}):

$$\text{Mass Activity} = \frac{J}{m}$$

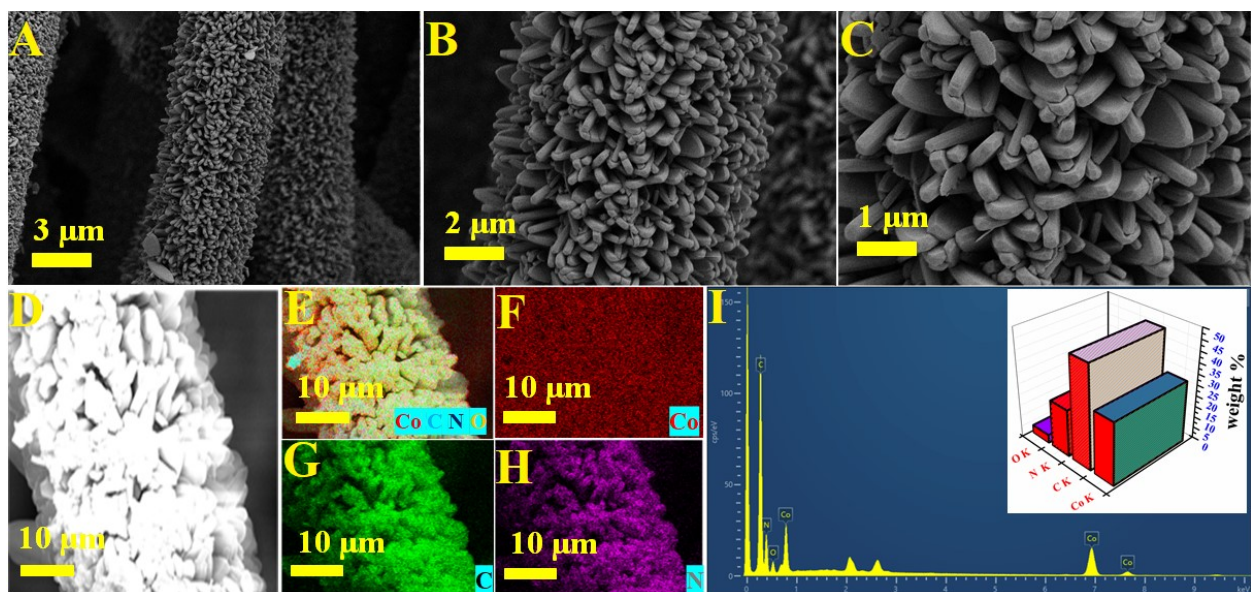


Figure S1. (A-C) Different magnification FESEM images of MOF Co nanoarrays@CC, (D) electron images, (E) corresponding elemental mapping images of Co (F), C (G), and N (H). (I) EDX spectrum and the inset image-related elemental contents of the MOF Co nanoarrays@CC.

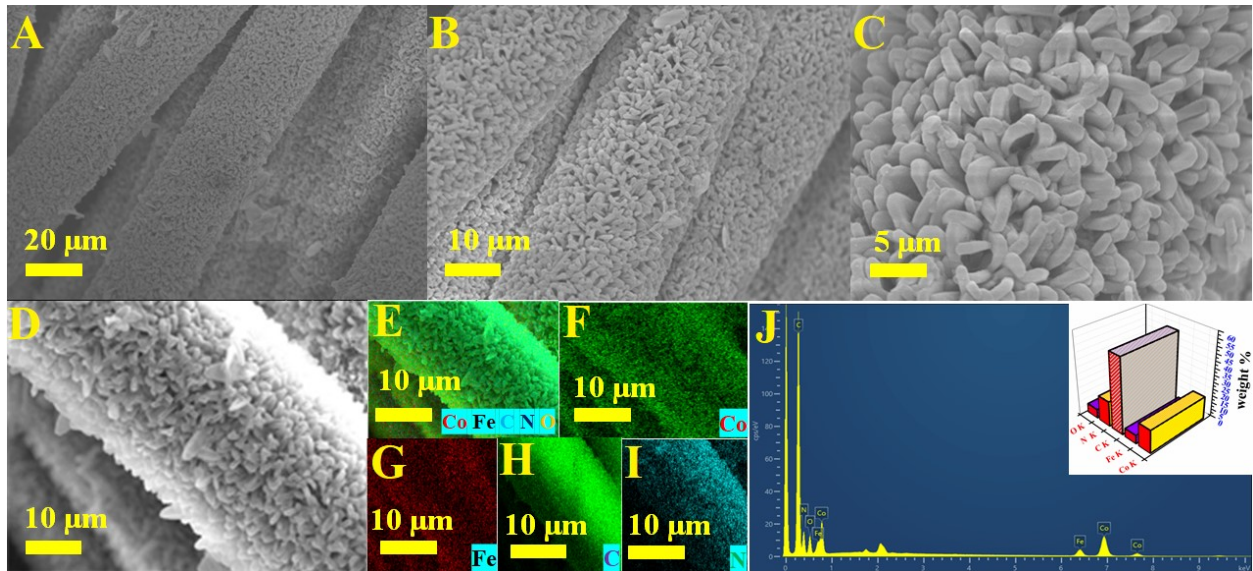


Figure S2. (A-C) Different magnification FESEM images of MOF CoPBA nanoarrays@CC, (D) electron images, (E) corresponding elemental mapping images of Co (F), Fe (G), C (H), and N (I). (J) EDX spectrum and the inset image-related elemental contents of the MOF CoPBA nanoarrays@CC.

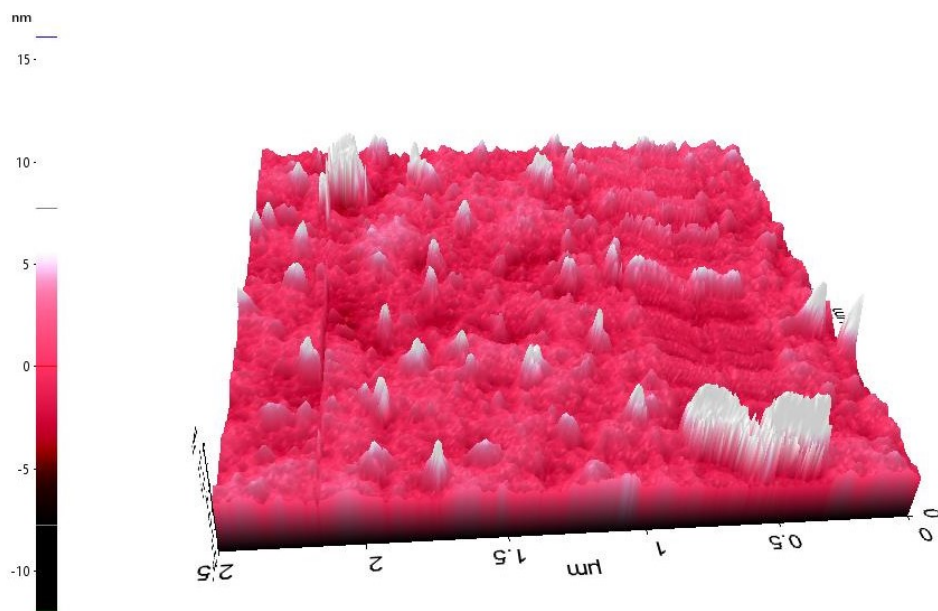


Figure S3. Three-dimensional surface topography AFM image Ru MOF CoFe nanoarrays @CC.

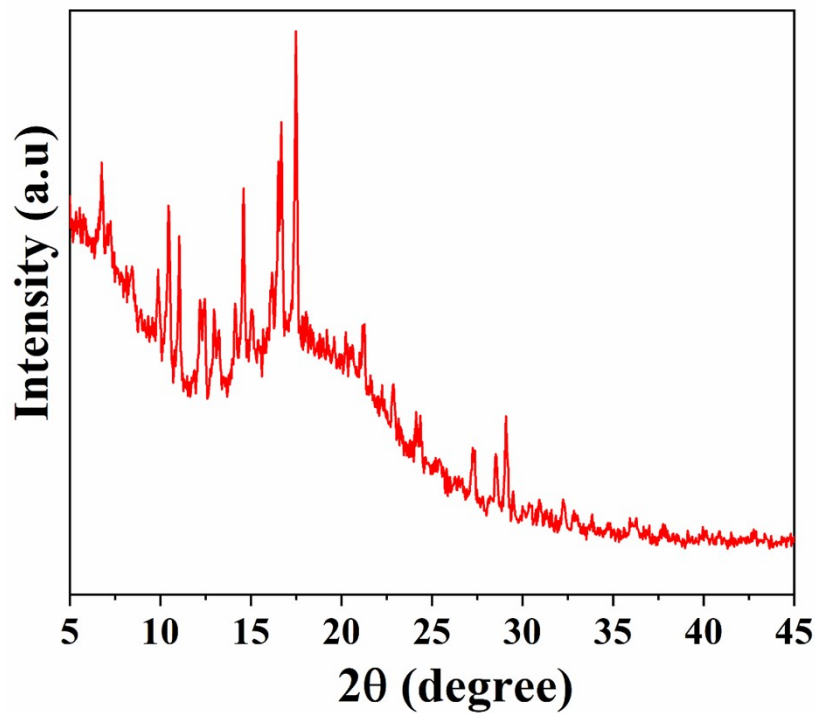


Figure S4. XRD patterns of MOF Co nanoarrays@CC

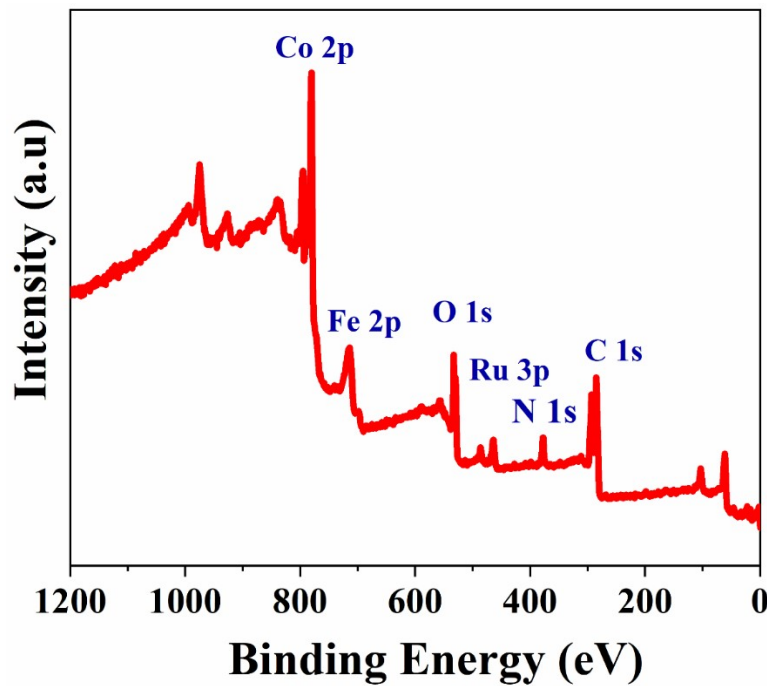


Figure S5. XPS survey spectrum of Ru MOF CoFe nanoarrays@CC

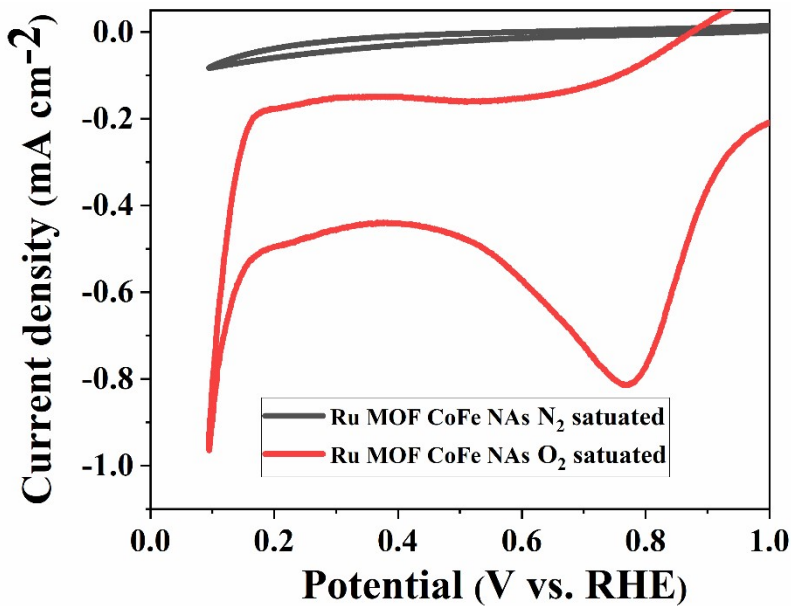


Figure S6. CV curve of Ru MOF CoFe nanoarrays@CC catalyst in N₂ and O₂ saturated 0.1 M KOH solution.

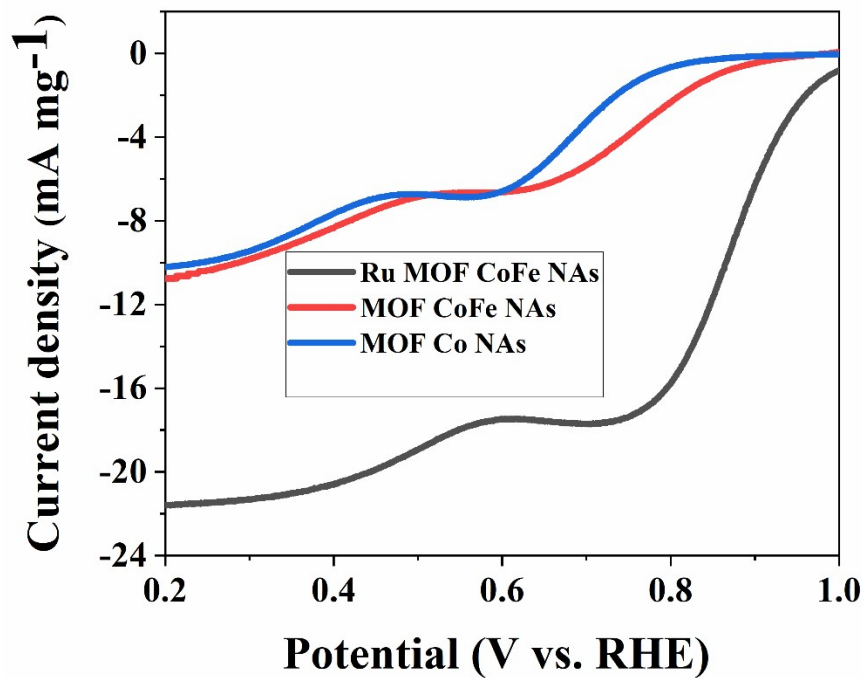


Figure. S7. RDE curves of Ru MOF CoFe nanoarrays@CC, (C) MOF CoFe nanoarrays@CC, and (E) MOF Co nanoarrays@CC in O₂-saturated 0.1 M KOH solution at a sweep rate of 5 mV s⁻¹.

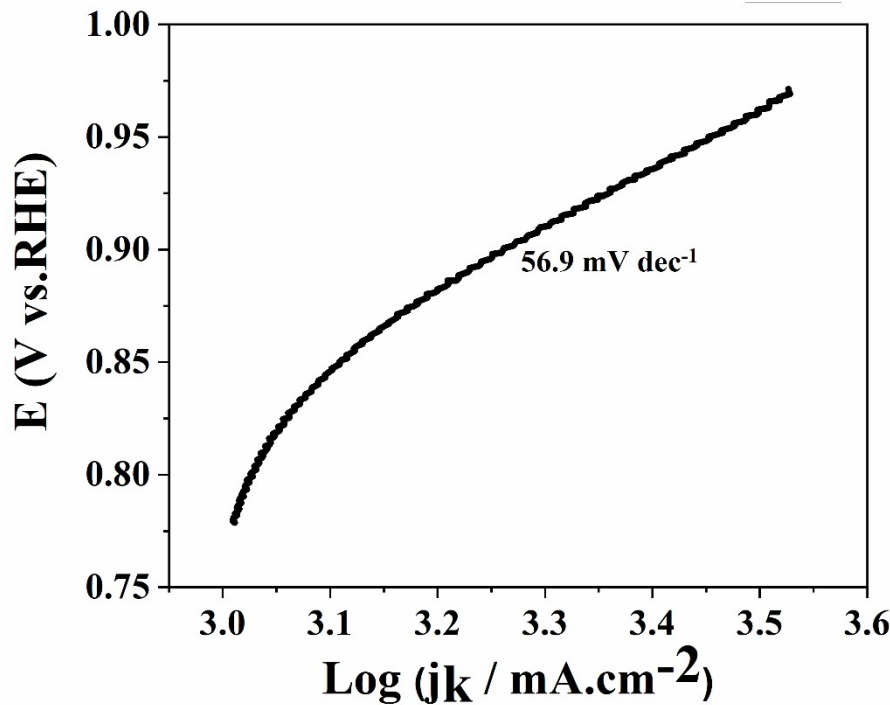


Figure S8. Tafel plot of Pt/C

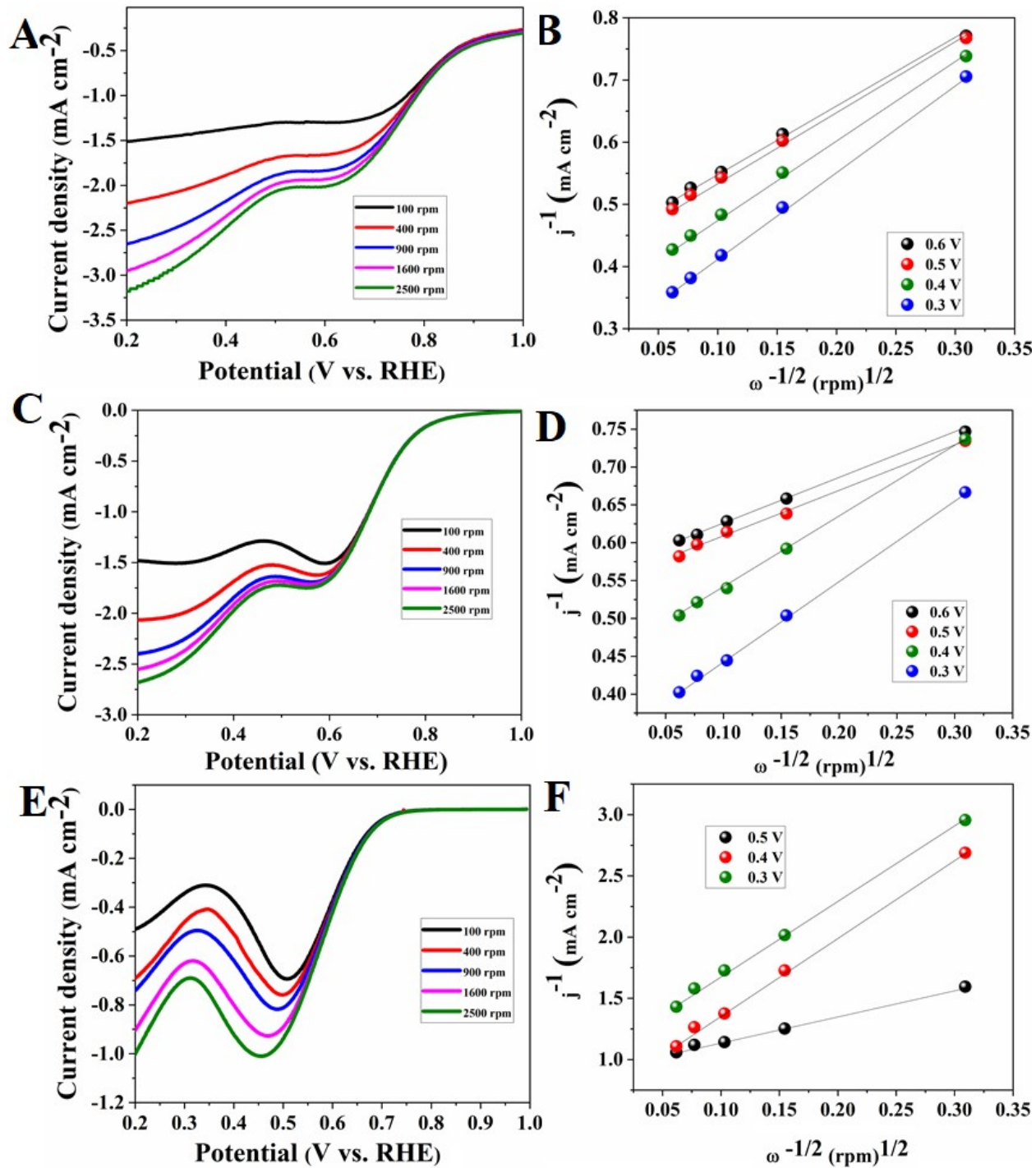


Figure S9. LSV curves of (A) MOF CoFe nanoarrays@CC, (C) MOF Co nanoarrays@CC, and (E) Bare GCE in O₂-saturated 0.1 M KOH solution at rotation rates from 100 to 2500 rpm. Related K-L plots of (B) MOF CoFe nanoarrays@CC, (D) MOF Co nanoarrays@CC, and (F) Bare GCE measured at the different potentials.

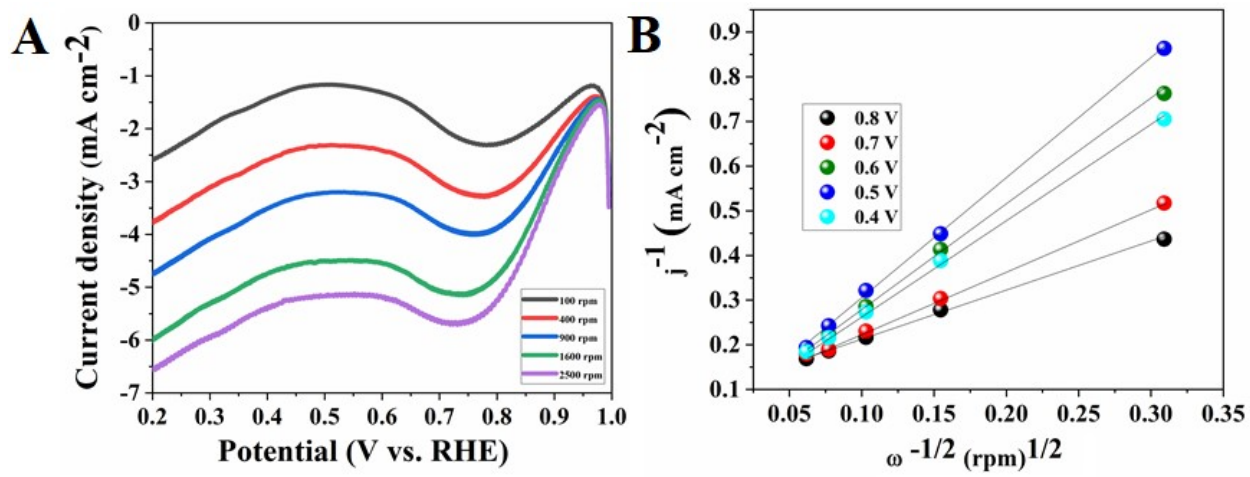


Figure S10. LSV curves of (A) Pt/C in O₂-saturated 0.1 M KOH solution at rotation rates from 100 to 2500 rpm. Related K-L plots of Pt/C measured at the different potentials.

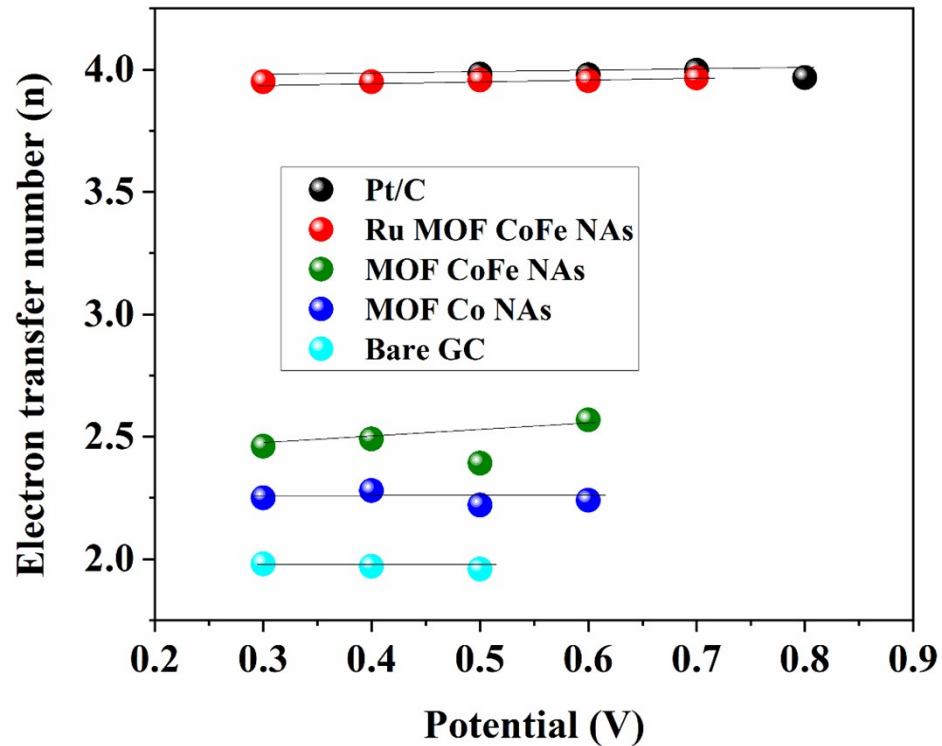


Figure S11. Electron transfer numbers were calculated at various potentials from KL plots for Pt/C, Ru MOF CoFe nanoarrays@CC, MOF CoFe nanoarrays@CC, MOF Co nanoarrays@CC, and bare GCE.

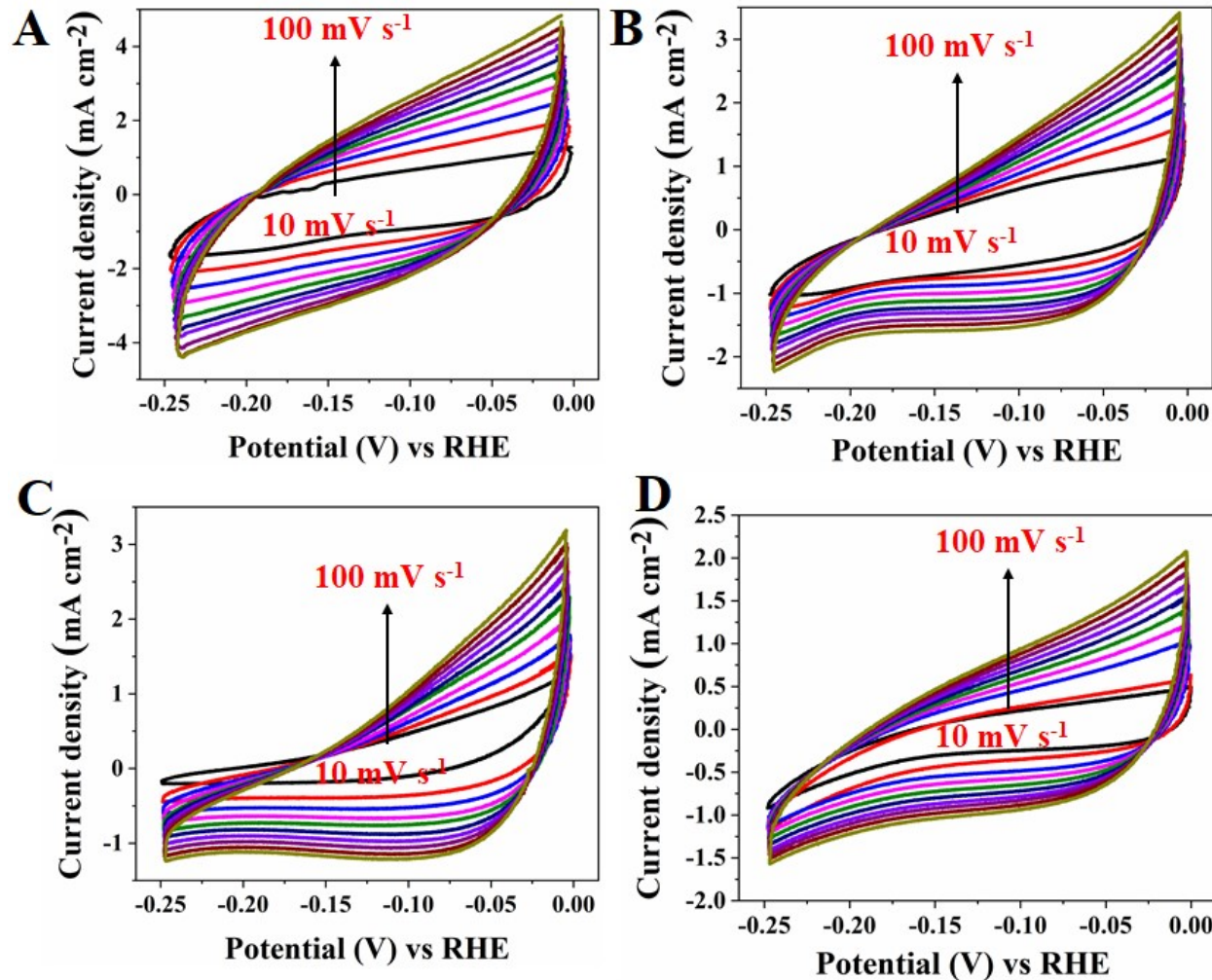


Figure S12. HER catalysts CV curves with different sweep rates from 10 to 100 mV s^{-1} (A) Ru MOF CoFe nanoarrays@CC, (B) MOF CoPBA nanoarrays@CC, (C) MOF Co nanoarrays@CC and (D) bare CC.

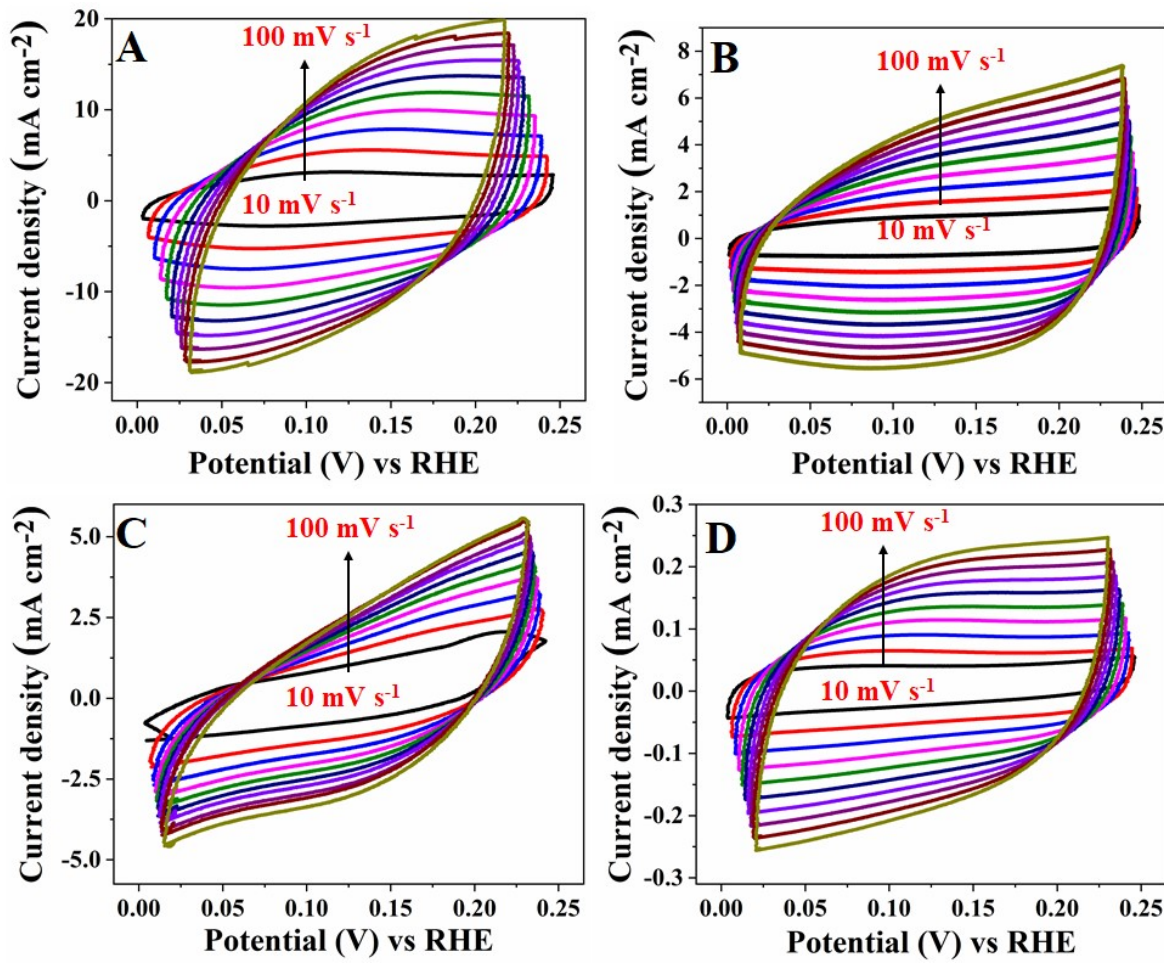


Figure S13. OER catalysts CV curves with different sweep rates from 10 to 100 mV s^{-1} (A) Ru MOF CoFe nanoarrays@CC, (B) MOF CoPBA nanoarrays@CC, (C) MOF Co nanoarrays@CC and (D) bare CC.

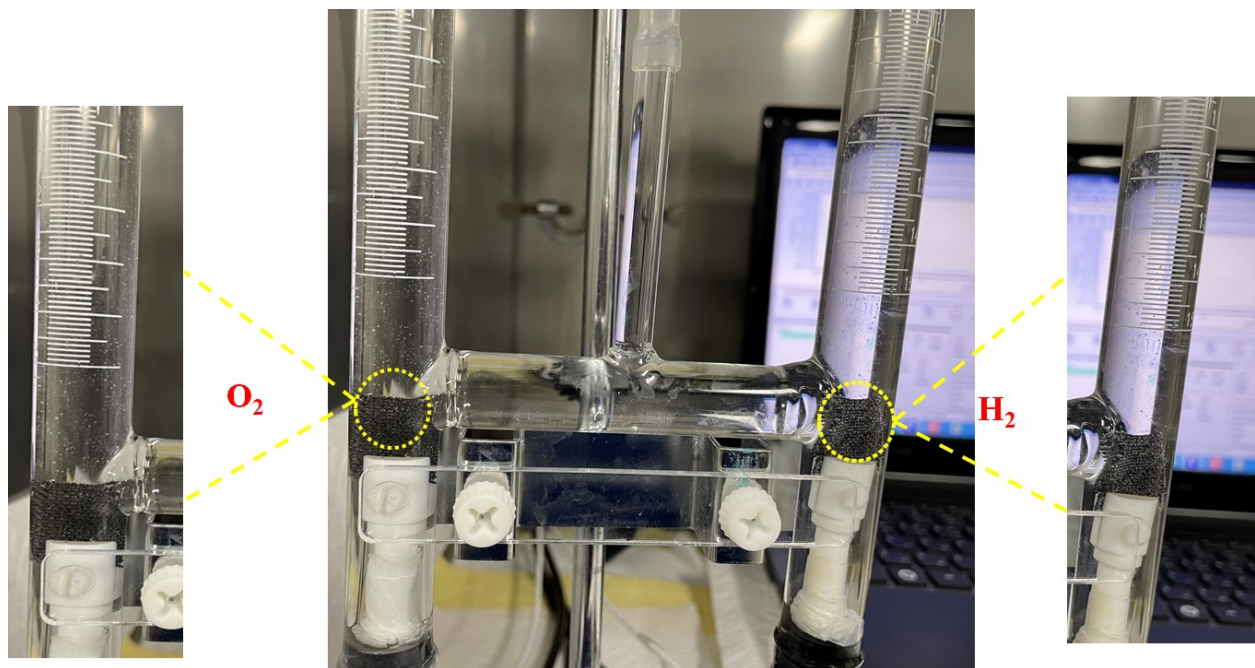


Figure S14: Digital photographic images of O₂ (anode) and H₂ (cathode) liberated in overall water splitting device.

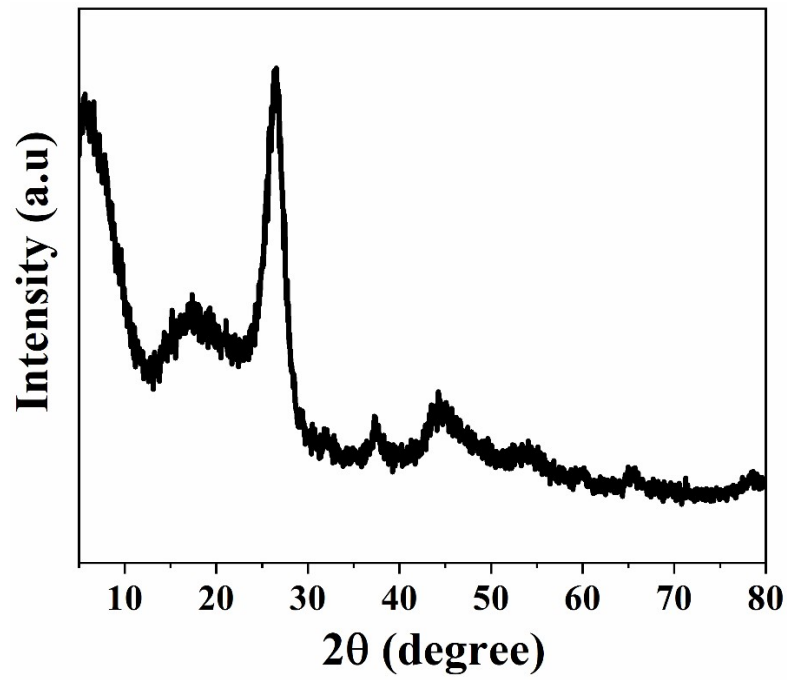


Figure S15. PXRD of Ru MOF CoFe nanoarrays catalyst after electrochemical cycle in 1 M KOH electrolyte.

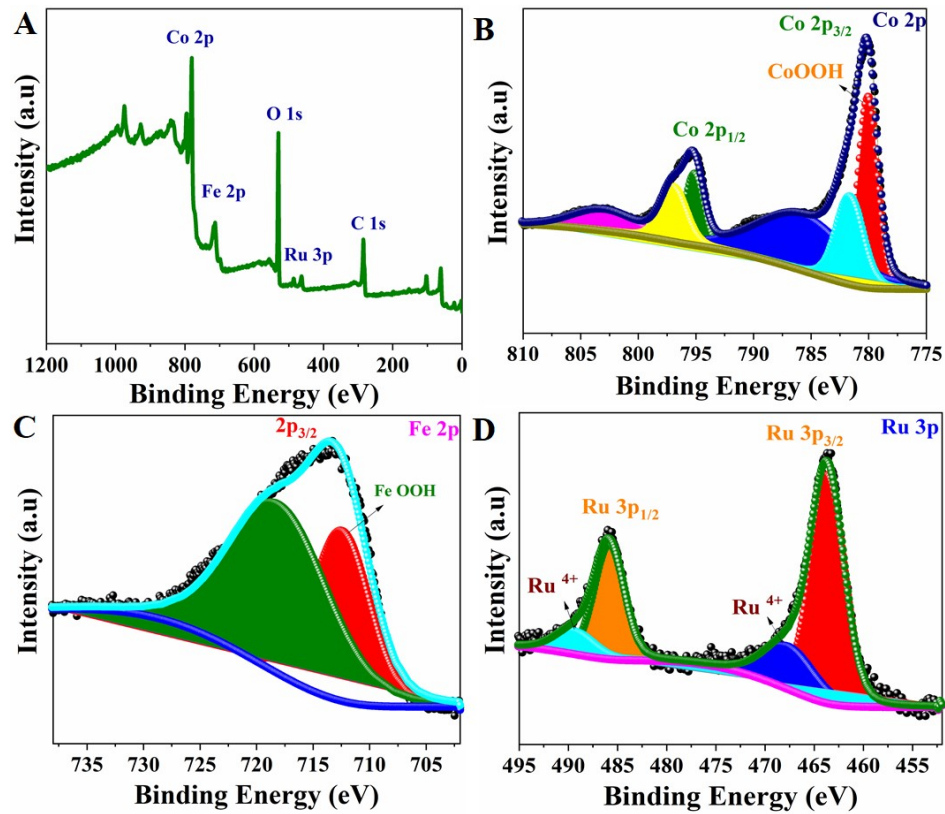


Figure S16. PXPS survey spectrum (A). High-resolution PXPS spectra of (B) Co 2p, (C) Fe 2p, and (D) Ru 3p of Ru MOF CoFe nanoarrays catalyst after electrochemical cycle.

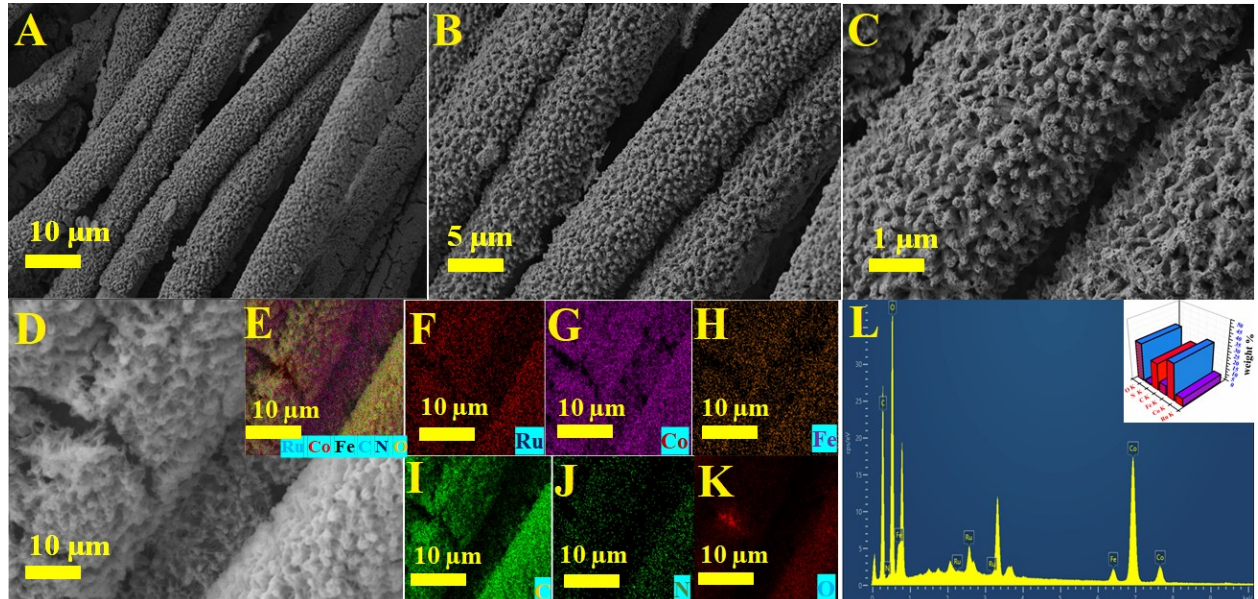


Figure S17. (A-C) Low and high magnification FESEM images of Ru MOF CoFe nanoarrays. (D) electron image and (E) elemental mapping images of Ru (F), Co (G), Fe (H), C (I), N (J), and O

(K). (L) EDX spectrum and inset image corresponding elemental composition images of Ru MOF CoFe nanoarrays in 1 M KOH solution observed after cyclic stability analysis.

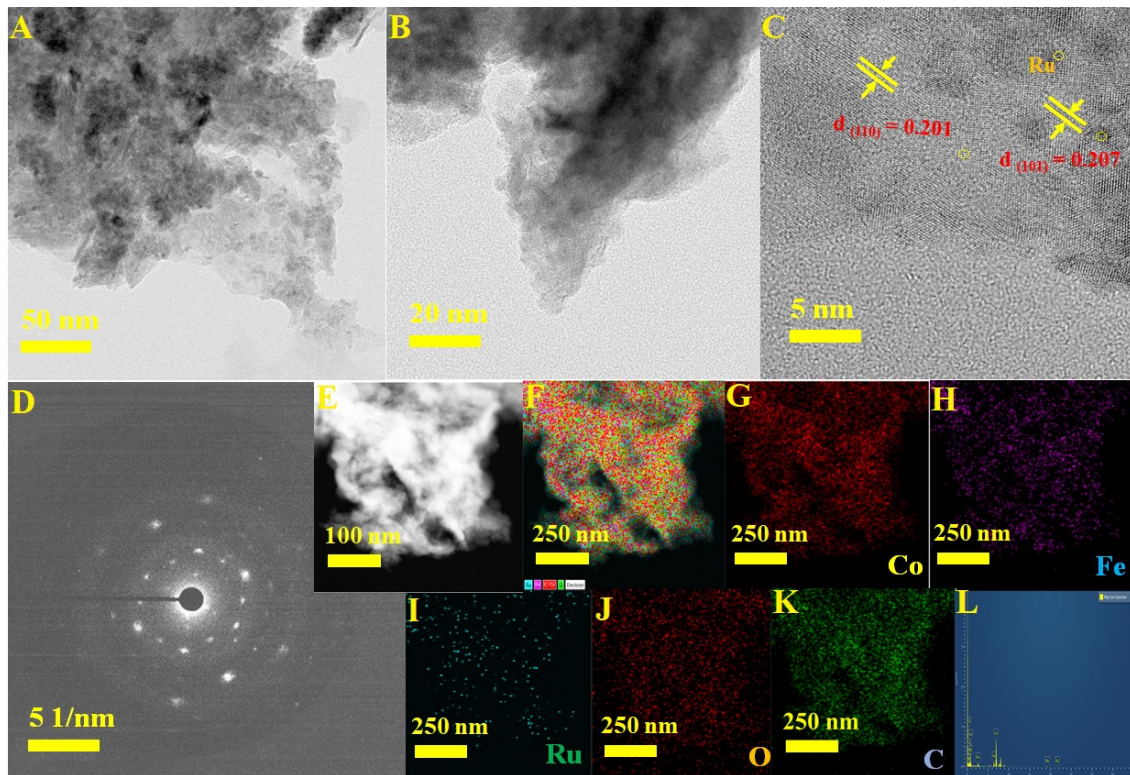


Figure S18. (A, B) TEM images, (C) HRTEM image, (D) SAED, (E) electron image, and (F) corresponding elemental mapping of (G) Co, (H) Fe, (I) Ru, (J) O, (K) C, and (L) TEM EDX spectrum of Ru MOF CoFe nanoarrays catalyst in 1 M KOH solution obtained after cyclic stability study.

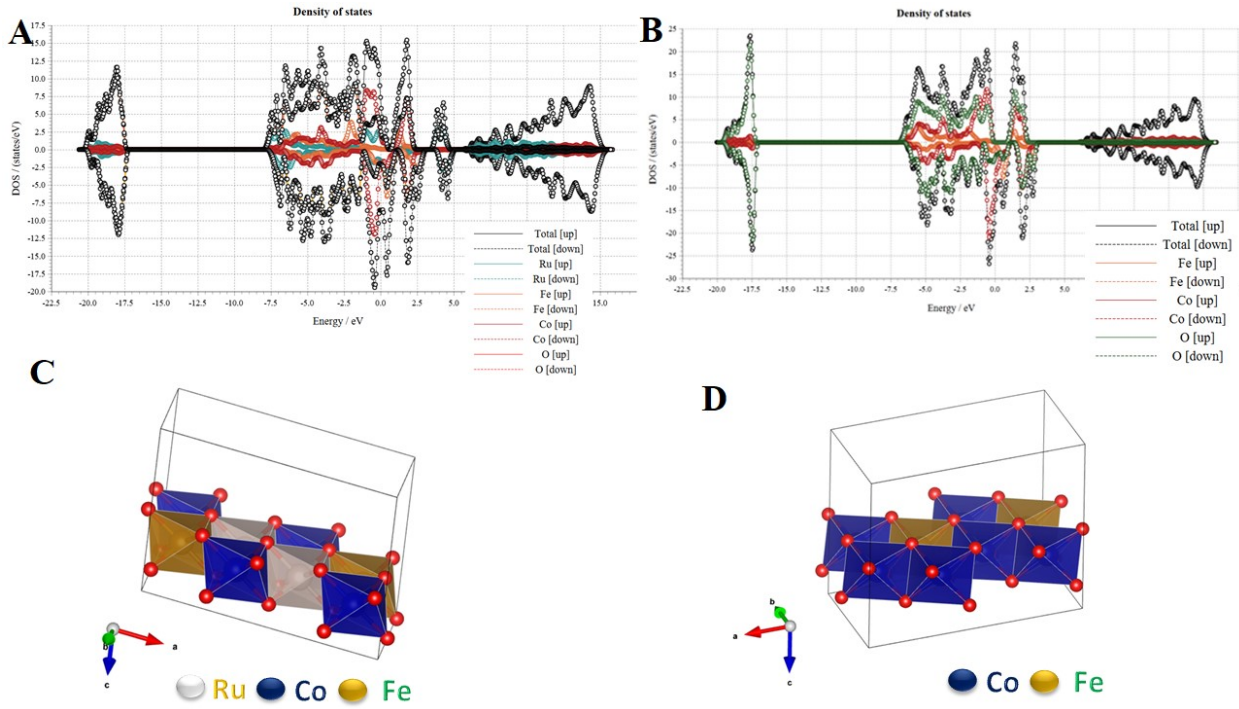


Figure S19. (A) DOS of Ru incorporated CoFe nanostructure, (B) DOS of CoFe nanostructure. (C) Crystal structure of Ru incorporated CoFe nanostructure, (D) crystal structure of CoFe nanostructure.

Table S1. Ru MOF CoFe nanoarrays and variously reported catalysts for HER, OER, and overall water splitting performance.

Bifunctional catalyst	Electrolytes	η at 10 mA cm ⁻² /mV		Tafel slope /mV dec ⁻¹		Two electrode Cell Voltage /V	References
		HER	OER	HER	OER		
Ru ₂ Ni ₂ SNs/C	1.0 M KOH	40	310	23	75	1.58	S1
Ru-NiFeP/NF	1.0 M KOH	105	179	67.5	58.6	1.48	19
FeCoNiP@NC	1.0 M KOH	187	266	52.2	35.6	1.73	S2

CoFeNx HNAs	1.0 M KOH	259	200	60.04	57.6	1.592	S3
NiFe LDHs	1.0 M KOH	210	240	—	—	1.7	S4
Fe-CoP UNSSs/NF	1.0 M KOH	67	166	48.88	65.89	1.47	S5
Fe _{0.27} Co _{0.73} P/N F	1.0 M KOH	186	251	60.5	59.1	1.68	S6
CoFe LDH-F	1.0 M KOH	166	260	116	47	1.63	S7
NiSe/NF	1.0 M KOH	96	270	120	64	1.63	S8
Co _{0.17} Fe _{0.79} P/N C	1.0 M KOH	139	299	64	44	1.66	S9
ONPPGC/ OCC	1.0 M KOH	446	410	154	83	1.66	S10
Cu/NiFe LDH	1.0 M KOH	116	199	58.9	27.8	1.56	S11
PPy/FeTCPP/ Co	1.0 M KOH	270	390	83	61	-	S12
Co ₁ Fe ₁ Mo _{1.8} O NM@NF	1.0 M KOH	157	210	112	32	1.68	S13
Co ₃ Fe ₇ @CN Ss	1.0 M KOH	181	301	124.8	38.59	1.61	S14
Au doped Co-Ni hydroxide	1.0 M KOH	200	340	92	54	1.733	S15
Fe-Ni alloy nanoparticles encapsulated in NDCHN	1.0 M KOH	201	270	133	63.9	1.701	S16
Co/NBC-900	1.0 M KOH	117	302	146	70	1.68	S17
CoPS@NPS- C	1.0 M KOH	191	326	106	98	1.62	S18
Fe–Co chalcogenoph	1.0 M KOH	260	365	62	49	1.59	S19

osphates							
Ru MOF CoFe nanoarrays	1.0 M KOH	50	220	46.5	49.7	1.49	This work

References

- S1 J. Ding, Q. Shao, Y. Feng, and X. Huang, *Nano Energy*, 2018, **47**, 1–7.
- S2 J. Sun, S. Li, Q. Zhang, and J. Guan, *Sustain. Energy Fuels*, 2020, **4**, 4531–4537.
- S3 D. Li, Y. Xing, R. Yang, T. Wen, D. Jiang, W. Shi and S. Yuan, *ACS Appl. Mater. Interfaces*, 2020, **12**, 29253–29263.
- S4 J. Luo, J. H. Im, M. T. Mayer, M. Schreier, M. K. Nazeeruddin, N. G. Park, S. D. Tilley, H. J. Fan and M. Grätzel, *Science (80-.)*, 2014, **345**, 1593–1596.
- S5 Y. Li, F. Li, Y. Zhao, S. N. Li, J. H. Zeng, H. C. Yao, and Y. Chen, *J. Mater. Chem. A*, 2019, **7**, 20658–20666.
- S6 C. Lin, P. Wang, H. Jin, J. Zhao, D. Chen, S. Liu, C. Zhang, and S. Mu, *Dalt. Trans.*, 2019, **48**, 16555–16561.
- S7 P. F. Liu, S. Yang, B. Zhang, and H. G. Yang, *ACS Appl. Mater. Interfaces*, 2016, **8**, 34474–34481.
- S8 C. Tang, N. Cheng, Z. Pu, W. Xing and X. Sun, *Angew. Chemie - Int. Ed.*, 2015, **54**, 9351–9355.
- S9 J. Chen, Y. Zhang, H. Ye, J. Q. Xie, Y. Li, C. Yan, R. Sun and C. P. Wong, *ACS Appl. Energy Mater.*, 2019, **2**, 2734–2742.
- S10 J. Lai, S. Li, F. Wu, M. Saqib, R. Luque, and G. Xu, *Energy Environ. Sci.*, 2016, **9**, 1210–1214.
- S11 L. Yu, H. Zhou, J. Sun, F. Qin, F. Yu, J. Bao, Y. Yu, S. Chen, and Z. Ren, *Energy Environ. Sci.*, 2017, **10**, 1820–1827.

- S12 J. Yang, X. Wang, B. Li, L. Ma, L. Shi, Y. Xiong and H. Xu, *Adv. Funct. Mater.*, 2017, **27**, 1606497.
- S13 L. Pei, Y. Song, M. Song, P. Liu, H. Wei, B. Xu, J. Guo, and J. Liang, *Electrochim. Acta*, 2021, **368**, 137651.
- S14 W. Yaseen, N. Ullah, M. Xie, W. Wei, Y. Xu, M. Zahid, C. J. Oluigbo, B. A. Yusuf and J. Xie, *Int. J. Hydrogen Energy*, 2021, **46**, 5234–5249.
- S15 U. K. Sultana, J. D. Riches, and A. P. O'Mullane, *Adv. Funct. Mater.*, 2018, **28**, 1804361.
- S16 L. Zhang, J. S. Hu, X. H. Huang, J. Song, and S. Y. Lu, *Nano Energy*, 2018, **48**, 489–499.
- S17 M. R. Liu, Q. L. Hong, Q. H. Li, Y. Du, H. X. Zhang, S. Chen, T. Zhou and J. Zhang, *Adv. Funct. Mater.*, 2018, **28**, 1804361.
- S18 Y. Hu, F. Li, Y. Long, H. Yang, L. Gao, X. Long, H. Hu, N. Xu, J. Jin and J. Ma, *J. Mater. Chem. A*, 2018, **6**, 10433–10440.
- S19 J. Tong, C. Li, L. Bo, X. Guan and Y. Wang, *Int. J. Hydrogen Energy*, 2020, **46**, 3354–3364.